Unconventional Josephson signatures of Majorana bound states

Liang Jiang[1], David Pekker[1], Jason Alicea[2], Gil Refael[1], Yuval Oreg,[3]and Felix von Oppen[4]

[1]*Department of Physics, California Institute of Technology, Pasadena, California 91125, USA*
[2] *Department of Physics and Astronomy, University of California, Irvine, CA 92697*
[3]*Department of Condensed Matter Physics, Weizmann Institute of Science, Rehovot, 76100, Israel and*
[4]*Dahlem Center for Complex Quantum Systems and Fachbereich Physik,*
Freie Universität Berlin, 14195 Berlin, Germany

A junction between two topological superconductors containing a pair of Majorana fermions exhibits a 'fractional' Josephson effect, 4π periodic in the superconductors' phase difference. An additional fractional Josephson effect, however, arises when the Majoranas are spatially separated by a superconducting barrier. This new term gives rise to a set of Shapiro steps which are essentially absent without Majorana modes and therefore provides a unique signature for these exotic states.

Majorana fermions comprise the simplest and likely most experimentally accessible non-Abelian anyon. An unambiguous demonstration of their non-Abelian exchange statistics would be a great triumph for condensed matter physics, as this phenomenon reflects one of the most spectacular manifestations of emergence. Furthermore, non-Abelian excitations provide the foundation behind topologically protected quantum computation [1, 2], with Majorana fermions playing a crucial role in prototype devices [3–7]. In the solid-state context, Majorana modes were originally perceived as zero-energy states bound to vortices in p-wave superconductors [8], and therefore are also associated with quasi-particles in the Moore-Read state [9]. More recent proposals employ topological insulators [10–12], half-metals in proximity to superconductors [13–15], as well as spin-orbit-coupled quantum wells [16, 17] and nanowires [18–21] to stabilize these elusive particles. Signatures of Majorana fermions appear in tunneling spectra and noise [22, 23], and more strikingly through interference effects [24, 25].

Josephson effects provide yet another important experimental signature of Majorana fermions. Kitaev first predicted that a pair of Majoranas fused across a junction formed by two topological superconducting wires generates a Josephson current [26]

$$I = \frac{e}{\hbar} J_M \sin\left(\frac{\phi_\ell - \phi_r}{2}\right), \qquad (1)$$

which exhibits a remarkable 4π periodicity in the superconducting phase difference $\phi_\ell - \phi_r$ between the left and right wires. In stark contrast to ordinary Josephson currents, this contribution reflects tunneling of *half* of a Cooper pair across the junction. Such a 'fractional' Josephson effect was later established in other systems supporting Majorana modes [10, 11, 18, 19, 27], and in direct junctions between p-wave superconductors [28]. In this manuscript we demonstrate that two topological superconductors bridged by an ordinary superconductor with phase ϕ_m generically support a second kind of un-

conventional Josephson effect with an associated current

$$I' = \frac{e}{\hbar} J_Z \sin\left(\frac{\phi_\ell + \phi_r}{2} - \phi_m\right), \qquad (2)$$

in the right or left superconductors, and twice that in the middle. This contribution arises solely from the fusion of spatially-separated Majoranas across the junction, and represents processes whereby a Cooper pair in the middle region splinters, with half entering the left and half entering the right topological superconductor. We will derive this emergent term in 1d Majorana-supporting systems, and propose several ways of measuring its effects.

This novel Josephson coupling is derived most simply in a 1d Kitaev chain. Consider a junction with Hamiltonian $H = H_\ell + H_r + \delta H$, where the left/right superconductors are described by p-wave-paired spinless fermions $c_{\alpha,x}$ ($\alpha = \ell,\, r$) hopping on an N-site chain [26],

$$H_\alpha = -\sum_{x=1}^{N-1}(tc^\dagger_{\alpha,x}c_{\alpha,x+1} + \Delta e^{i\phi_\alpha}c_{\alpha,x}c_{\alpha,x+1} + h.c.). \quad (3)$$

Eq. (3) adiabatically connects to realistic Majorana-supporting quantum wire Hamiltonians [18, 19, 29], and therefore describes their universal properties as well. Following Kitaev, we express the spinless fermions in terms of two Majorana operators via $c_{\alpha,x} = \frac{1}{2}e^{-i\frac{\phi_\alpha}{2}}(\gamma^\alpha_{B,x} + i\gamma^\alpha_{A,x})$. When $t = \Delta$, Eq. (3) maps onto a dimerized Majorana chain: $H_\alpha = -it\sum_{x=1}^{N-1}\gamma^\alpha_{B,x}\gamma^\alpha_{A,x+1}$. The explicit absence of $\gamma^\alpha_{A,1}$ and $\gamma^\alpha_{B,N}$ in the Hamiltonians indicates the presence of zero-energy Majorana modes localized at the ends of each superconductor in the junction.

Let us now couple the two superconductors through

$$\delta H = -t_m(c^\dagger_{\ell,N}c_{r,1} + h.c.) - \Delta_m(e^{i\phi_m}c_{\ell,N}c_{r,1} + h.c.), \quad (4)$$

where the two terms describe tunneling and Cooper pairing across the junction. These couplings combine the zero-energy Majorana modes residing at the junction into a finite-energy Andreev bound state. Focusing on these zero-energy modes, one can write $c_{\ell,N} \to \frac{1}{2}e^{-i\phi_\ell/2}\gamma^\ell_{B,N}$ and $c_{r,1} \to i\frac{1}{2}e^{-i\phi_r/2}\gamma^r_{A,1}$, and define an ordinary fermion
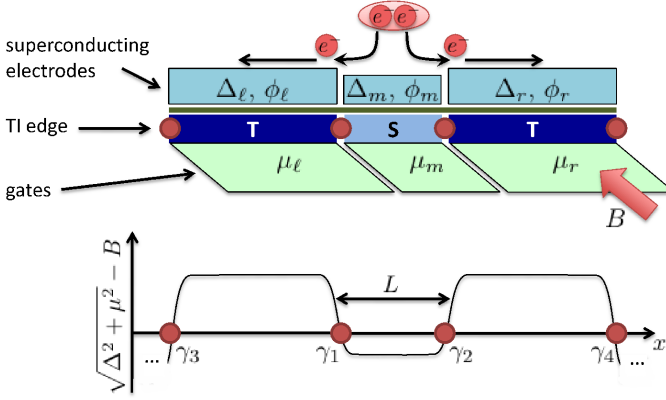
FIG. 1: Topological insulator edge subjected to a magnetic field B and sandwiched by gates and superconducting electrodes. Majorana modes (red circles) localize at domain walls where the gap $E_{gap} = |\sqrt{\mu^2 + \Delta^2} - B|$ vanishes and the argument in the absolute value changes sign. When the middle region is a trivial superconductor (S), and the sides form a topological phase (T), the novel J_Z term in Eq. (5), with current $\propto \sin(\frac{\phi_\ell + \phi_r}{2} - \phi_m)$, accompanies the usual the fractional Josephson effect. This splits a Cooper pair in the middle electrode into two single electrons, injected via the two Majorana states in each topological segment. The same effect appears in spin-orbit-coupled wires in a T-S-T configuration.

operator $f^\dagger = \frac{1}{2}(\gamma_{B,N}^\ell + i\gamma_{A,1}^r)$; δH then becomes

$$\delta H \rightarrow (2f^\dagger f - 1)\{J_M \cos[(\phi_\ell - \phi_r)/2]$$
$$+ J_Z \cos[(\phi_\ell + \phi_r)/2 - \phi_m]\}. \quad (5)$$

with $J_M = \frac{t_m}{2}$ and $J_Z = \frac{\Delta_m}{2}$. Since the current in region s is given by $\frac{2e}{\hbar} \frac{\partial \langle \delta H \rangle}{\partial \phi_s}$, the fermion tunneling t_m gives rise to the fractional Josephson effect of Eq. (1), while pairing Δ_m across the junction produces the Josephson current in Eq. (2). Note that the sign of either current is dictated by the occupation number for the f fermion, and hence can be used as a readout method for qubit states encoded by the Majoranas [11, 29].

A more quantitative understanding is obtained by considering more realistic models. Let us consider Majoranas localized on a topological insulator edge in proximity to a superconductor and subjected to a magnetic field [10]; a very similar analysis applies to quantum wires. In the Nambu spinor basis $\Psi^T = (\psi_\uparrow, \psi_\downarrow, \psi_\downarrow^\dagger, -\psi_\uparrow^\dagger)$, the Bogoliubov-de Gennes Hamiltonian for this system is

$$\mathcal{H} = v\hat{p}\sigma^z\tau^z - \mu\tau^z + \Delta\left(\cos\phi\tau^x - \sin\phi\tau^y\right) + B\sigma^x, \quad (6)$$

with v the edge-state velocity, $\hat{p}$ the momentum, B the Zeeman energy, and σ^a and τ^a Pauli matrices acting in the spin and particle-hole sectors, respectively. We allow the chemical potential μ, pairing amplitude Δ, and superconducting phase ϕ, to vary spatially.

Majorana states arise at interfaces between topological (T) and trivial (S) regions of the edge [10]. With μ,

Δ, and ϕ uniform the quasi-particle gap is $E_{gap} = |B - \sqrt{\Delta^2 + \mu^2}|$. When $\sqrt{\Delta^2 + \mu^2} > B$ the edge is gapped by proximity-induced superconductivity and forms a topological phase closely related to that of Kitaev's model described above [10]. In the trivial phase $\sqrt{\Delta^2 + \mu^2} < B$, and the magnetic field dominates the gap. We will study the T-S-T domain sequence of Fig. 1, which localizes Majoranas γ_1 at $x = 0$ and γ_2 at $x = L$. Each of the three regions, ℓ, r, m, couples to a superconductor imparting proximity strength $\Delta_{\ell/m/r}$ and phase $\phi_{\ell/m/r}$, and has a chemical potential $\mu_{\ell/m/r}$ controlled by separate gates. (The main difference in the quantum wire case is that there creating the T-S-T domain structure needed to observe the unconventional Josephson effects discussed here requires the reversed criteria: $\sqrt{\Delta^2 + \mu^2} < B$ in the outer regions and $\sqrt{\Delta^2 + \mu^2} > B$ in the middle region.)

The Majorana-related Josephson effects result from hybridization between γ_1 and γ_2. When γ_1 and γ_2 are far apart ($L \rightarrow \infty$), they constitute exact zero-energy modes, and their wave functions decay exponentially in region $s = \ell, m, r$ with *two* characteristic lengths:

$$\lambda_{s\pm} = \frac{v}{|\Delta_s \pm \sqrt{B^2 - \mu_s^2}|} \quad (7)$$

(we assume $\mu_s < B$). For finite L, however, $\gamma_{1,2}$ combine into a finite-energy state with creation operator $f^\dagger = \frac{1}{2}(\gamma_1 + i\gamma_2)$. Roughly, each Majorana perceives the interface localizing the other Majorana as a perturbation, yielding a hybridization which is suppressed as a weighted sum of two decaying exponentials. This hybridization is again described by Eq. (5), with $J_{M/Z} = \frac{1}{2}\left(J_+ e^{-L/\lambda_{m+}} \pm J_- e^{-L/\lambda_{m-}}\right)$. An explicit calculation (see supp. material) for the symmetric setup, $\mu_\ell = \mu_r \equiv \mu$, $\Delta_\ell = \Delta_r \equiv \Delta > \Delta_m$ and $\mu_m = 0$ yields

$$J_+ = J_- \approx \frac{2\Delta}{\frac{\Delta(B+\Delta)+\mu^2}{\Delta^2+\mu^2-B^2} + \frac{B\Delta}{B^2-\Delta_m^2}}. \quad (8)$$

When $\Delta_m = 0$ and the middle region is normal—which is the setup typically studied [10, 18]—$J_Z = 0$ and hence only the Josephson term in Eq. (1) appears. Turning on $\Delta_m \neq 0$ yields a nonzero J_Z, and the second Josephson term in Eq. (2). Furthermore, since both J_Z and J_M are dominated by the slowest decay length, they will generically be of the same order. For a quantitative estimate, consider the parameters $\mu_m = 0$, $\mu_{l,r} = E$, $\Delta_m = E$, $\Delta_{l,r} = \sqrt{8}E$, $B = 2E$ with energy scale $E = 0.1$meV. Assuming an edge velocity $v = 10^4$m/s, for this choice we obtain $\lambda_{m+} \approx 22$nm, $\lambda_{m-} \approx 66$nm, and $J_\pm \approx 0.12$meV. The effect then peaks at $L \approx 50$nm, which yields $J_Z \approx 0.022$ meV and $I_Z = \frac{e}{\hbar}J_Z \approx 5.3$nA.

These Josephson effects are simplest to understand conceptually when two additional Majoranas, $\gamma_{3,4}$, straddle the T segments of the edge as shown in Fig. 1. Let us define fermion operators $f_A = \frac{1}{2}(\gamma_1 + i\gamma_3)$ and $f_B = \frac{1}{2}(\gamma_2 + i\gamma_4)$, and assume that the corresponding

occupation numbers are initially $n_A = 1$ and $n_B = 0$. We will further employ a 'perturbative' perspective and promote the superconducting phases to quantum operators conjugate to the Cooper pair number. One can then see that the Majorana operators in the term $J_M(2f^\dagger f - 1)\exp(i\frac{\phi_r - \phi_\ell}{2}) = iJ_M\gamma_1\gamma_2\exp(i\frac{\phi_r - \phi_\ell}{2})$ hop a single fermion across the S region, changing the state of the edge from $(n_A, n_B) = (1,0)$ to $(0,1)$. At the same time, the exponential passes a charge e from side to side. The combination of these processes makes the term gauge invariant. The persistent superconducting current limit in this case is apparent when we consider an additional tunneling event which restores the parities of the T segments, moving a fermion back to the left but with a Cooper pair hopping to the right. A similar perspective clarifies the role of the J_Z term—the Majoranas in $iJ_Z\gamma_1\gamma_2\exp\left[i\left(\frac{\phi_r + \phi_\ell}{2} - \phi_m\right)\right]$ also change the parity of the two T segments, while the exponent removes a Cooper pair from the middle region and adds charge e to each T region (see Fig. 1).

Next, we discuss the crucial issue of measuring the new Josephson term in Eq. (2). The first and most direct possibility involves manipulating independently the phase differences $\phi_\ell - \phi_m \equiv \Phi_L$ and $\phi_m - \phi_r \equiv \Phi_R$, e.g., by inserting different fluxes in the two loops in Fig. 2a (ignoring the voltage sources in the figure). By tuning $\Phi_L = -\Phi_R$ in a symmetric junction, one can probe the J_Z Josephson term (driving current $J_Z\sin\Phi_L$ on the middle electrode) while canceling the J_M term. Such measurements, however, are highly challenging—they require careful flux control; the Majorana-related Josephson current must be disentangled from the conventional 2π periodic contributions; and the measurement must be concluded before the parity of the two Majoranas changes.

A potentially more promising measurement scheme relies on Shapiro steps. In a regular Josephson junction, Shapiro steps arise from a combination of a dc voltage V_{dc} and an ac voltage $V_{ac}\sin\omega t$, which together generate a current $I = I_J\sin[\phi_0 + 2eV_{dc}t/\hbar - (2eV_{ac}/\hbar\omega)\cos\omega t]$. Naively, this current averages to zero because of the constantly winding phase. This is not the case, however, when $2eV_{dc}/\hbar = n\omega$ for some integer n—here a dc current component exists, producing a step in the V vs. I plot for the junction [30, 31]. For the fractional Josephson term in Eq. (1), the 4π periodicity leads to Shapiro steps when $2eV_{dc}/\hbar = 2n\omega$, corresponding to even Shapiro steps of a regular Josephson junction. The halved periodicity, if established, could provide a smoking-gun signature for Majorana modes. An inevitable conventional Josephson current, however, 'fills in' the missing steps, making it difficult to disentangle these contributions [28].

The following three-leg Shapiro-step measurement circumvents this problem and targets the Josephson term of Eq. (2). As shown in Fig. 2a, we envision a dc voltage applied to the left leg so that $\phi_\ell = 2eV_{dc}t/\hbar$,
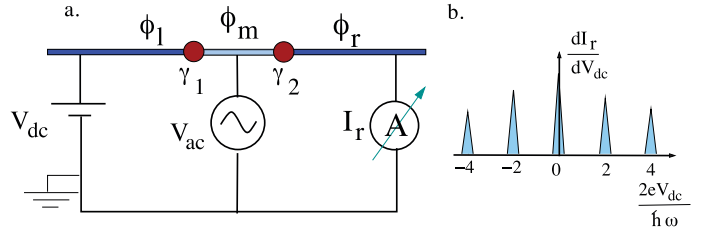

FIG. 2: Three-leg Shapiro-step measurement scheme. (a) We envision applying a dc voltage V_{dc} to the left superconducting electrode and an ac voltage with angular frequency ω in the left loop (which we model as an ac voltage applied to the middle electrode). A measurement of the dc current I_r in the right electrode will then reveal Shapiro steps stemming from the Majorana modes when the ac Josephson frequency $2eV_{dc}/\hbar$ equals an *even* harmonic of ω. (b) Sketch of dI_r/dV_{dc} indicating the predicted Shapiro steps—note the crucial absence of odd-harmonic peaks, which would appear in a conventional Shapiro-step measurement.

while an ac voltage applied to the middle leg sets $\phi_m = -(2eV_{ac}/\hbar\omega)\cos\omega t$. Since the new Josephson term induces current in all three legs, a current measurement on the right lead will find Shapiro steps emerging only when

$$2eV_{dc}/\hbar = 2n\omega \qquad (9)$$

as illustrated in Fig. 2b, without any odd-harmonic steps. This non-local measurement is insensitive to any parasitic two-phase Josephson terms, and therefore automatically eliminates most competing processes. Furthermore, it bears the advantage of being a fast dynamic measurement (since Josephson frequencies are typically in the GHz regime), which reduces its sensitivity to temporal fluctuations of the Majorana-state occupations.

To verify the approximation methods used and to confirm the prominence of the J_Z term in the three-leg Shapiro measurement, we also numerically analyzed the Josephson effects in a topological insulator edge. Figure 3 shows that our analytical results [e.g., Eq. (8)] indeed agree very well with the exact numerical calculation. We also explored additional current contributions such as $\delta I\sin(\phi_L + \phi_R - 2\phi_m)$, which could obscure the Majorana signature by producing unwanted odd-harmonic Shapiro steps. This term is independent of the Majorana modes, and can instead arise from conventional Bogoliubov states in the junction. In the limit of small pairing and tunneling over the middle segments, such a term reflects a high-order process. Numerically, we find that it is suppressed by at least an order of magnitude compared to the Majorana J_Z contribution in the regime where J_Z is substantial, i.e., when L is of order $\lambda_{m\pm}$.

By considering the full edge spectrum (including the Andreev bound states and continuum states exactly), we obtained the total Josephson energy of the domain configuration in Fig. 1:

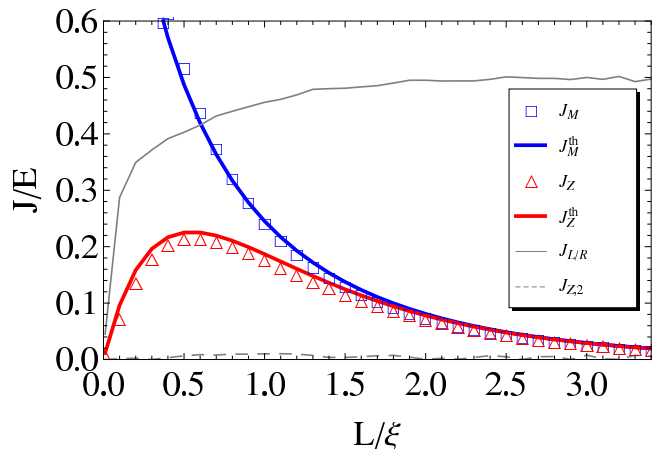$$E_{\text{tot}} \approx J_L\cos(\phi_\ell - \phi_m) + J_R\cos(\phi_r - \phi_m)$$

FIG. 3: Numerically determined coefficients of conventional Josephson couplings ($J_{L/R}$), Majorana-induced terms ($J_{M/Z}$), and second harmonic of the J_Z term ($J_{Z,2}$). Our analytical estimates of J_M^{th} and J_Z^{th} agree well with numerics. The energy unit is E and the length unit is $\xi = v/E$. The parameters are $\mu_{l,r} = E, \mu_m = 0, \Delta_{l,r} = \sqrt{8}E, \Delta_m = E$, and $B_{l,r} = B_m = 2E$. The characteristic lengths are $\lambda_{m+} = \xi/3$ and $\lambda_{m-} = \xi$. For $E = 0.1$meV and $v = 10^4$m/s, the length unit is $\xi = 66$nm and the maximum current is $I_Z = \frac{e}{\hbar} J_Z \approx 5.3$nA.

$$+ \ J_M \cos[(\phi_\ell - \phi_r)/2] + J_Z \cos[(\phi_\ell + \phi_r)/2 - \phi_m]$$
$$+ \ \sum_{n=2}^{\infty} J_{Z,n} \cos[n((\phi_\ell + \phi_r)/2 - \phi_m)] + \cdots \qquad (10)$$

Here $J_{L/R}$ are conventional Josephson terms (to which the three-leg measurement is insensitive), $J_{M/Z}$ are the Majorana-induced contributions, and $J_{Z,n}$ denote the (unwanted) higher harmonics of the J_Z term. As Fig. 3 illustrates, J_M dominates for $L \ll \lambda_{m+}$, while for $\lambda_{m-} \gtrsim L \gtrsim \lambda_{m+}$ the J_Z term becomes comparable, enabling the three-leg Shapiro-step measurement. The higher harmonics $J_{Z,n}$ are at least an order of magnitude smaller than J_Z in this regime and can be neglected. For $L \gg \lambda_{m-}$ the Majorana signatures are strongly suppressed as expected.

In this manuscript, we explored a new Josephson effect that arises when a pair of Majorana fermions fuse across a junction formed by two topological superconductors separated by an ordinary superconductor. The Majoranas in this setup enable Cooper pairs injected into the barrier superconductor to 'splinter' into the left and right legs of the junction—a process which would ordinarily be prohibited at low energies. While Majorana modes can also give rise to a novel fractional Josephson effect in T-normal-T junctions, we argued that an important advantage of our setup is that here one can more readily isolate the Majorana-mediated Josephson current through Shapiro-step measurements. The experiments we proposed could provide a relatively simple and unambiguous detection scheme for Majorana fermions, and

may also serve as a practical readout mechanism for qubit states encoded by these particles.

[1] A. Y. Kitaev, Annals of Physics **303**, 2 (2003).
[2] C. Nayak, S. H. Simon, A. Stern, M. Freedman, and S. Das Sarma, Rev. Mod. Phys. **80**, 1083 (2008).
[3] S. Das Sarma, M. Freedman, and C. Nayak, Phys. Rev. Lett. **94**, 166802 (2005).
[4] P. Bonderson, M. Freedman, and C. Nayak, Annals of Physics **324**, 787 (2009).
[5] F. Hassler, A. R. Akhmerov, C.-Y. Hou, and C. W. J. Beenakker, New Journal of Physics **12**, 125002 (2010).
[6] L. Jiang, C. L. Kane, and J. Preskill, Phys. Rev. Lett. **106**, 130504 (2011).
[7] P. Bonderson and R. M. Lutchyn, Phys. Rev. Lett. **106**, 130505 (2011).
[8] G. Volovik, JETP Letters **70**, 609 (1999).
[9] N. Read and D. Green, Phys. Rev. B **61**, 10267 (2000).
[10] L. Fu and C. L. Kane, Phys. Rev. Lett. **102**, 216403 (2009).
[11] L. Fu and C. L. Kane, Phys. Rev. Lett. **100**, 096407 (2008).
[12] A. Cook and M. Franz, arXiv:1105.1787.
[13] M. Duckheim and P. W. Brouwer, Phys. Rev. B **83**, 054513 (2011).
[14] P. A. Lee (2009), arxiv:0907.2681.
[15] H. Weng, G. Xu, H. Zhang, S.-C. Zhang, X. Dai, and Z. Fang, ArXiv e-prints (2011), 1103.1930.
[16] J. D. Sau, R. M. Lutchyn, S. Tewari, and S. Das Sarma, Phys. Rev. Lett. **104**, 040502 (2010).
[17] J. Alicea, Phys. Rev. B **81**, 125318 (2010).
[18] R. M. Lutchyn, J. D. Sau, and S. Das Sarma, Phys. Rev. Lett. **105**, 077001 (2010).
[19] Y. Oreg, G. Refael, and F. von Oppen, Phys. Rev. Lett. **105**, 177002 (2010).
[20] L. Jiang, T. Kitagawa, J. Alicea, A. R. Akhmerov, D. Pekker, G. Refael, J. I. Cirac, E. Demler, M. D. Lukin, and P. Zoller, Phys. Rev. Lett. **106**, 220402 (2011).
[21] L. Mao, M. Gong, E. Dumitrescu, S. Tewari, and C. Zhang, arXiv:1105.3483.
[22] C. J. Bolech and E. Demler, Phys. Rev. Lett. **98**, 237002 (2007).
[23] K. T. Law, P. A. Lee, and T. K. Ng, Phys. Rev. Lett. **103**, 237001 (2009).
[24] P. Bonderson, A. Kitaev, and K. Shtengel, Phys. Rev. Lett. **96**, 016803 (2006).
[25] A. Stern and B. I. Halperin, Phys. Rev. Lett. **96**, 016802 (2006).
[26] A. Y. Kitaev, Physics-Uspekhi **44**, 131 (2001).
[27] P. A. Ioselevich and M. V. Feigel'man, Phys. Rev. Lett.

106, 077003 (2011).

[28] H.-J. Kwon, K. Sengupta, and V.M. Yakovenko, Eur. Phys. J. B **37**, 349 (2004).

[29] J. Alicea, Y. Oreg, G. Refael, F. von Oppen, and M. P. A. Fisher, Nature Phys. **7**, 412 (2011).

[30] S. Shapiro, Phys. Rev. Lett. **11**, 80 (1963).

[31] M. Tinkham, *Introduction to superconductivity* (McGraw Hill, New York, 1996), 2nd ed.

[32] G. D. Mahan, *Many-particle physics* (Kluwer Academic/Plenum Publishers, New York, 2000), 3rd ed.

[33] E. Akkermans, A. Auerbach, J. E. Avron, and B. Shapiro, Phys. Rev. Lett. **66**, 76 (1991).

SUPPLEMENTARY MATERIAL

PERTURBATIVE CALCULATION

Let us pursue here a detailed calculation of the Josephson coupling across the Majorana junction described in Fig. 1. We will first find the wave functions of the Majorana states localized on each domain wall, ignoring the existence of the other interface. We will denote these states as $|L\rangle$ and $|R\rangle$. Next, we follow the usual procedure for finding tight-binding states and Hamiltonians. We first calculate the overlap matrix, $M_{\alpha\beta} = \langle\alpha|\beta\rangle$ with $\alpha, \beta = L, R$, and the Hamiltonian matrix within this subspace, $h_{\alpha\beta} = \langle\alpha|\mathcal{H}|\beta\rangle$. It is easy to see that the approximate hybridization Hamiltonian is then given by

$$H_{maj} = M^{-1/2} h M^{-1/2}. \tag{11}$$

Single Majorana solution at $x = L$. We first solve for the zero-energy eigenstates of the Hamiltonian (6) with parameters:

$$\Delta(x) = \Delta_r \Theta(x - L) + \Delta_m(1 - \Theta(x - L)) \\ \mu(x) = \mu_r \Theta(x - L) + \mu_m(1 - \Theta(x - L)) \tag{12}$$

The solution has the same form on the two sides of the domain wall, but with different parameters. We denote the side of the domain with the index s being $s = r, m$ for right or middle. By squaring the Hamiltonian and looking for momentum values yielding zero energy states, we find two imaginary momenta on each side, which correspond to the spatial decay constants $\lambda_{s\pm}^{-1}$ given by Eq. (7). The wave function associated with each side of the domain is:

$$|r\rangle = \Psi_s(x) = R_{s+}\psi_{s+} e^{-\frac{|x-L|}{\lambda_{s+}}} + R_{s-}\psi_{s-} e^{-\frac{|x-L|}{\lambda_{s-}}}. \tag{13}$$

with $R_{s\pm}$ being four complex numbers determining the amplitude of the wave functions corresponding to the two decay lengths, and with $\psi_{s\pm}$ being four, four-dimensional vectors, which when $\phi_s = 0$ are given by:

$$\psi_{m\pm} = \begin{pmatrix} 1 \\ e^{-i\zeta_m} \\ \pm i \\ \mp i e^{-i\zeta_m} \end{pmatrix}, \quad \psi_{r\pm} = \begin{pmatrix} 1 \\ e^{\pm i\zeta_r} \\ i \\ -i e^{\pm i\zeta_r} \end{pmatrix} \tag{14}$$

with $\exp(i\zeta_s) = \frac{\mu_s + i\sqrt{B^2 - \mu_s^2}}{B}$, for $s = \ell, r, m$. These solutions are the building blocks for each Majorana state. In order to obtain what the wave function becomes when ϕ_s (the phases of the superconducting electrodes) deviate from zero, we can apply the rotations: $\hat{U}_\phi = \exp\left(i\frac{\phi}{2}\tau_z\right)$ such that:

$$\psi_{s\pm}^{(\phi_s)} = \hat{U}_{\phi_s}\psi_{s\pm}. \tag{15}$$

Obtaining the Majorana solution follows from matching the boundary condition of the solutions, and from them finding the coefficients $R_{s\pm}$.

To avoid the complicated expression that could arise in the most general case of Majorana coupling, we concentrate on the case where $\Delta_r = \Delta_\ell > \Delta_m$ and $\mu_r = \mu_\ell = \mu$ and $\mu_m = 0$. This choice does not constitute a substantial loss of generality, and is useful for grasping the results of our calculations. A straightforward but rather tedious calculation leads to the following solution for the amplitudes of the decaying waves of the right Majorana state under the above assumptions:

$$\begin{pmatrix} R_{m+} \\ R_{m-} \end{pmatrix} = \frac{2\sin\zeta_r}{1 + ie^{-i\zeta_r}} \begin{pmatrix} i\sin\left(\frac{\phi_r - \phi_m}{2}\right) \\ \cos\left(\frac{\phi_r - \phi_m}{2}\right) \end{pmatrix}, \\ \begin{pmatrix} R_{r+} \\ R_{r-} \end{pmatrix} = \begin{pmatrix} -\frac{1 + ie^{i\zeta_r}}{1 + ie^{-i\zeta_r}} \\ 1 \end{pmatrix}. \tag{16}$$

By symmetry, we can infer the structure of the left Majorana, which is localized about $x = 0$:

$$|L\rangle = \Psi_s^{(L)}(x) = L_{s+}\psi_{s+} e^{-\frac{|x|}{\lambda_{s+}}} + L_{s-}\psi_{s-} e^{-\frac{|x|}{\lambda_{s-}}}. \tag{17}$$

The amplitudes $L_{s\pm}$ also depend on the phases on the left and middle segment of the wire in a similar way:

$$\begin{pmatrix} L_{m+} \\ L_{m-} \end{pmatrix} = \frac{2\sin\zeta_\ell}{1 - ie^{i\zeta_\ell}} \begin{pmatrix} -i\sin\left(\frac{\phi_\ell - \phi_m}{2}\right) \\ \cos\left(\frac{\phi_\ell - \phi_m}{2}\right) \end{pmatrix}, \\ \begin{pmatrix} L_{\ell+} \\ L_{\ell-} \end{pmatrix} = \begin{pmatrix} -\frac{1 - ie^{-i\zeta_\ell}}{1 - ie^{i\zeta_\ell}} \\ 1 \end{pmatrix} \tag{18}$$

From the above results, and under the symmetric choice of parameters, we can compute the overlap matrix, $M_{\alpha\beta} = \langle\alpha|\beta\rangle$. Neglecting exponentially suppressed corrections, we obtain the following form:

$$M_{\alpha\beta} = v\delta_{\alpha\beta}\left[\frac{B + \Delta_m \cos(\phi_\alpha - \phi_m)}{2(B^2 - \Delta_m^2)} + \frac{\Delta_r(B + \Delta_r) + \mu^2}{2\Delta_r(\Delta_r^2 - B^2 + \mu^2)}\right], \tag{19}$$

with v being the spin-orbit velocity.

The coupling between the Majoranas could be calculated perturbatively by considering the two domain walls juxtaposed. For instance, while the left Majorana is an exact zero-energy eigenstate of the Hamiltonian

$$\mathcal{H}_L = \mathcal{H}_\ell \Theta(-x) + \mathcal{H}_m \Theta(x),$$

the existence of the right segment of the wire perturbs this wave function, with the perturbation potential being

$$V_r = (\mathcal{H}_r - \mathcal{H}_m)\theta(x - L).$$

Similarly, we can write $\mathcal{H} = \mathcal{H}_R + V_\ell$ with $V_\ell = (\mathcal{H}_\ell - \mathcal{H}_m)\theta(-x)$. This perturbation induces a hybridization matrix between the left Majorana and the right Majorana:

$$h = \begin{pmatrix} \langle L| V_r |L\rangle = 0 & \langle L| V_r |R\rangle \\ \langle R| V_r |L\rangle & \langle R| V_\ell |R\rangle = 0 \end{pmatrix}. \quad (20)$$

In our case,

$$V_r = [(\Delta_r \cos \phi_r - \Delta_m \cos \phi_m)\, \tau^x - \\ (\Delta_r \sin \phi_r - \Delta_m \sin \phi_m)\, \tau^y - \mu_r \tau_z]\, \Theta(x - L).$$

The perturbation matrix we obtain is:

$$h = iv e^{i\nu\epsilon_{\alpha\beta}} \epsilon_{\alpha\beta} \left[e^{-L/\lambda_+^m} \sin \frac{\phi_r - \phi_m}{2} \sin \frac{\phi_\ell - \phi_m}{2} \\ + e^{-L/\lambda_-^m} \cos \frac{\phi_r - \phi_m}{2} \cos \frac{\phi_\ell - \phi_m}{2} \right]. \quad (21)$$

with ν an unimportant phase.

We arrive at the final answer for the Josephson coupling using Eq. (11). The result indeed coincides with Eq. (5):

$$\mathcal{H}_{JM} = (2f^\dagger f - 1) \left[J_+ e^{-L/\lambda_+} \sin \frac{\phi_r - \phi_m}{2} \sin \frac{\phi_\ell - \phi_m}{2} \\ + J_- e^{-L/\lambda_-} \cos \frac{\phi_r - \phi_m}{2} \cos \frac{\phi_l - \phi_m}{2} \right] \\ = (2f^\dagger f - 1) \left(J_M \cos \frac{\phi_r - \phi_\ell}{2} + J_Z \cos \left(\frac{\phi_r + \phi_\ell}{2} - \phi_m \right) \right) \quad (22)$$

with the constants $J_\pm$ being:

$$J_+ = J_- \approx \frac{v}{\overline{M}_{rr}}. \quad (23)$$

where $\overline{M}_{rr} = v \left[\frac{B}{2(B^2 - \Delta_m^2)} + \frac{\Delta_r(B + \Delta_r) + \mu^2}{2\Delta_r(\Delta_r^2 - B^2 + \mu^2)} \right]$. is the average of the overlap matrix [Eq. (19)] diagonal elements, dropping the cosine term. The cosine term in the overlap will produce additional harmonics of the Majorana-Josephson term but will not qualitatively change the answer we obtained. The $J_\pm$ terms give rise to to the previously explored Majorana-Josephson term, Eq. (1) and to the new zipper term, Eq. (2).

NUMERICAL CALCULATION

We now detail the procedure of our numerical calculation. In the Nambu spinor basis $\Psi^T = (\psi_\uparrow, \psi_\downarrow, \psi_\downarrow^\dagger, -\psi_\uparrow^\dagger)$, the Bogoliubov-de Gennes Hamiltonian for this system is

$$\mathcal{H} = v\hat{p}\sigma^z\tau^z - \mu\tau^z + \Delta(\cos\phi\tau^x - \sin\phi\tau^y) + B\sigma^x, \quad (24)$$

with v the edge-state velocity, $\hat{p}$ the momentum, B the Zeeman energy, and σ^a and τ^a Pauli matrices acting in the spin and particle-hole sectors, respectively. We allow the chemical potential μ, pairing amplitude Δ, and superconducting phase ϕ, to vary spatially. In region s (with $s = l, m, r$), the parameters $(\mu, \Delta, \phi) = (\mu_s, \Delta_s, \phi_s)$ are constant. Without loss of generality, we assume $\phi_m = 0$ to be a reference of superconducting phase.

The Josephson effects in the TST junction has both bound states and continuum contributions. In the following, we first present the procedure to compute the exact interaction energy E between two Majoranas, and then provide the formalism to calculate the energy contribution from the continuum.

Bound state energy

For TST configuration, there are two Majoranas at interfaces between topological and trivial regions. The finite separation leads to a finite interaction energy $E = E_{int}$ between these two Majoranas, with spatial-dependent wave function $\Psi = \Psi(x)$ satisfying the equation

$$\mathcal{H}\Psi = E\Psi. \quad (25)$$

We will solve the interaction energy $E = E_{int}$ by matching the boundary condition of the wave function.

First, we replace the momentum operator $\hat{p}$ with $-i\frac{\partial}{\partial x}$, and obtain the linear differential equation associated with energy E

$$\frac{\partial}{\partial x}\Psi(x) = \mathbf{G}_E\Psi(x), \quad (26)$$

with 4×4 matrix

$$\mathbf{G}_E = i\frac{\mu}{v}\sigma^z + \frac{\Delta}{v}\sigma^z(\cos\phi\tau^y + \sin\phi\tau^x) - \frac{B}{v}\sigma^y\tau^z + i\frac{E}{v}\sigma^z\tau^z. \quad (27)$$

In region s (with $s = l, m, r$), the parameters $(\mu, \Delta, \phi) = (\mu_s, \Delta_s, \phi_s)$ are constant, and the matrix $G_E^{(s)}$ has eigensystem

$$\mathbf{G}_E^{(s)}\vec{u}_j^{(s)} = \kappa_j^{(s)}\vec{u}_j^{(s)} \quad (28)$$

with eigenvalues $\kappa_j^{(s)}$ and eigenvectors $\vec{u}_j^{(s)}$ for $j = 1, \cdots, 4$ and $s = l, m, r$.

Then, we expand the four-component wave function $\Psi(x)$ in terms of eigenvectors $\vec{u}_j^{(s)}$. We are interested in the localized state with $E < E_{gap}^{(l,r)}$. In the left region, there are two localized modes ($\text{Re}\kappa_{1,2}^{(l)} > 0$) and the two divergent modes ($\text{Re}\kappa_{3,4}^{(l)} < 0$). Similarly, in the right region, there are two localized modes ($\text{Re}\kappa_{1,2}^{(r)} < 0$) and the two divergent modes ($\text{Re}\kappa_{3,4}^{(r)} > 0$). The wave function with two localized Majoranas consists of localized modes

$$\Psi(x) = \begin{cases} \sum_{j=1,2} c_j^{(l)} e^{\kappa_j^{(l)}x} \vec{u}_j^{(l)} & \text{for } x \leq 0 \\ \sum_{j=1,2} c_j^{(r)} e^{\kappa_j^{(r)}(x-L)} \vec{u}_j^{(r)} & \text{for } x \geq L \end{cases}. \quad (29)$$
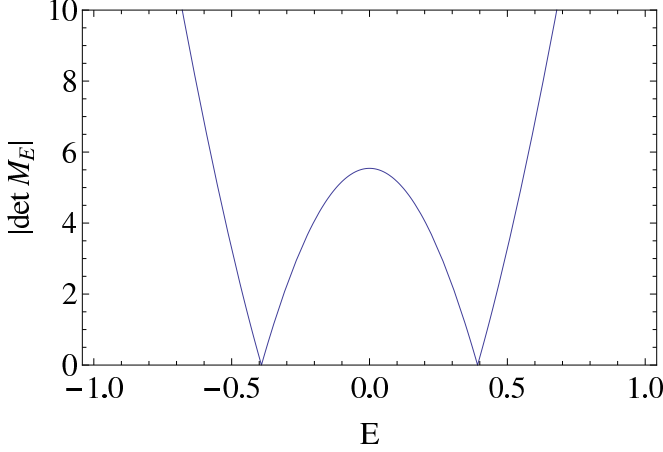
FIG. 4: The function $\det M_E$ vanishes when $E = \pm E_{int}$, which can be used to numerically find the interaction energy between the Majoranas.

In order to match the coefficients associated with left and right regions, we integrate the wavefunction over the middle region and obtain the condition

$$\sum_{j=1,2} c_j^{(r)} \vec{u}_j^{(r)} = \Psi(L) = e^{\mathbf{G}_E^{(m)} L} \Psi(0) = \sum_{j=1,2} c_j^{(l)} e^{\mathbf{G}_E^{(m)} L} \vec{u}_j^{(l)}, \quad (30)$$

which can be written as

$$\mathbf{M}_E \begin{pmatrix} c_1^{(l)} \\ c_2^{(l)} \\ c_1^{(r)} \\ c_2^{(r)} \end{pmatrix} = \begin{pmatrix} 0 \\ 0 \\ 0 \\ 0 \end{pmatrix} \quad (31)$$

with 4×4 matrix

$$\mathbf{M}_E = \left[\left(e^{\mathbf{G}_E^{(m)} L} \vec{u}_1^{(l)} \right) \; \left(e^{\mathbf{G}_E^{(m)} L} \vec{u}_2^{(l)} \right) \; \left(-\vec{u}_1^{(r)} \right) \; \left(-\vec{u}_2^{(r)} \right) \right]. \quad (32)$$

The necessary condition for non-zero solution is

$$\det \mathbf{M}_E = 0, \quad (33)$$

which can be used to numerically determine the interaction energy E_{int}. As illustrated in Fig. 4, the function $\det \mathbf{M}_E$ vanishes at $E = \pm E_{int}$. (There is a technical subtlety associated with the fact that $\mathbf{G}_E^{(l,r)}$ is *not* a Hermitian matrix. For some fixed values of E, the eigenvalues of $\mathbf{G}_E^{(l,r)}$ have multiplicity larger than one, and the eigenvector $\vec{u}_j^{(l,r)}$ might be a zero vector, which may also lead to spurious solutions with vanishing $\det \mathbf{M}_E$. This issue can be resolved by using a polynomial discriminant to identify and remove these spurious solutions.)

Continuum contribution

We now consider the energy contribution from the continuum. The continuum states can be characterized by the scattering matrix $\mathbf{S}_E = \mathbf{S}_E(\phi_l, \phi_r)$, which can be computed by matching the boundary conditions for all incoming and outgoing modes. Once we know the scattering matrix, we can use the Fumi's sum rule to compute the continuum contribution to the system energy [32, 33]

$$W(\phi_l, \phi_r) = \int_{E_{gap}}^{\infty} \frac{dE}{2\pi i} \ln\left[\det\left[\mathbf{S}_E(\phi_l, \phi_r)\right]\right]. \quad (34)$$

The continuum contribution consists of many Fourier components

$$W(\phi_l, \phi_r) = \frac{1}{2} \sum_{n_l, n_r = -\infty}^{\infty} W_{n_l, n_r} \cos(n_l \phi_\ell + n_r \phi_r) \quad (35)$$

with $W_{n_l, n_r} = W_{-n_l, -n_r}$. Then conventional Josephson terms are $J_{L/R} = W_{1,0}$ and $W_{0,1}$, and the even harmonics of the zipper terms are $J_{Z,2n} = W_{n,n}$. In the following, we provide the formalism to compute the scattering matrix $S_E(\phi_l, \phi_r)$.

For energy $E > E_{gap}^{(l,r)}$, there are the propagating modes $(\mathrm{Re}\kappa_j^{(l,r)} = 0)$, with momentum $p_j^{(l,r)} = \mathrm{Im}\kappa_j^{(l,r)}$. Suppose there are four incoming modes $\left(\vec{u}_1^{(l)}, \vec{u}_2^{(l)}, \vec{u}_1^{(r)}, \vec{u}_2^{(r)}\right)$ with $p_{1,2}^{(l)} > 0$ and $p_{1,2}^{(r)} < 0$, and four outgoing modes $\left(\vec{u}_3^{(l)}, \vec{u}_4^{(l)}, \vec{u}_3^{(r)}, \vec{u}_4^{(r)}\right)$ with $p_{3,4}^{(l)} < 0$ and $p_{3,4}^{(r)} > 0$. The wave function can be written as a linear combination of all these modes

$$\Psi(x) = \begin{cases} \sum_{j=1,\cdots,4} c_j^{(l)} e^{\kappa_j^{(l)} x} \vec{u}_j^{(l)} & \text{for } x \leq 0 \\ \sum_{j=1,\cdots,4} c_j^{(r)} e^{\kappa_j^{(r)} (x-L)} \vec{u}_j^{(r)} & \text{for } x \geq L \end{cases}. \quad (36)$$

In order to match the coefficients associated with left and right regions, we integrate the wavefunction over the middle region and obtain the condition $\Psi(L) = e^{\mathbf{G}_E^{(m)} L} \Psi(0)$. The relation between the amplitudes of incoming and outgoing modes is

$$\mathbf{M}_{E,in} \begin{pmatrix} c_1^{(l)} \\ c_2^{(l)} \\ c_1^{(r)} \\ c_2^{(r)} \end{pmatrix} = \mathbf{M}_{E,out} \begin{pmatrix} c_3^{(l)} \\ c_4^{(l)} \\ c_3^{(r)} \\ c_4^{(r)} \end{pmatrix} \quad (37)$$

with 4×4 matrices

$$\mathbf{M}_{E,in} = \left[\left(e^{\mathbf{G}_E^{(m)} L} \vec{u}_1^{(l)} \right) \; \left(e^{\mathbf{G}_E^{(m)} L} \vec{u}_2^{(l)} \right) \; \left(-\vec{u}_1^{(r)} \right) \; \left(-\vec{u}_2^{(r)} \right) \right], \quad (38)$$

$$\mathbf{M}_{E,out} = \left[\left(-e^{\mathbf{G}_E^{(m)} L} \vec{u}_3^{(l)} \right) \; \left(-e^{\mathbf{G}_E^{(m)} L} \vec{u}_4^{(l)} \right) \; \left(\vec{u}_3^{(r)} \right) \; \left(\vec{u}_4^{(r)} \right) \right]. \quad (39)$$

The scattering relation is

$$
\mathbf{S}_E
\begin{pmatrix}
\left(p_1^{(l)}\right)^{1/2} c_1^{(l)} \\
\left(p_2^{(l)}\right)^{1/2} c_2^{(l)} \\
\left(p_1^{(r)}\right)^{1/2} c_1^{(r)} \\
\left(p_2^{(r)}\right)^{1/2} c_2^{(r)}
\end{pmatrix}
=
\begin{pmatrix}
\left(-p_3^{(l)}\right)^{1/2} c_3^{(l)} \\
\left(-p_4^{(l)}\right)^{1/2} c_4^{(l)} \\
\left(-p_3^{(r)}\right)^{1/2} c_3^{(r)} \\
\left(-p_4^{(r)}\right)^{1/2} c_4^{(r)}
\end{pmatrix}
\tag{40}
$$

with scattering matrix

$$
\boxed{\mathbf{S}_E = \mathbf{P}_{out}^{1/2} \cdot \mathbf{M}_{E,out}^{-1} \cdot \mathbf{M}_{E,in} \cdot \mathbf{P}_{in}^{-1/2},}
\tag{41}
$$

where $\mathbf{P}_{in} = \mathrm{Diag}\left[p_1^{(l)}, p_2^{(l)}, p_1^{(r)}, p_2^{(r)}\right]$ and $\mathbf{P}_{out} = -\mathrm{Diag}\left[p_3^{(l)}, p_4^{(l)}, p_3^{(r)}, p_4^{(r)}\right]$. The requirement of conservation of current is

$$
\sum_j p_j^{(l)} \left|c_j^{(l)}\right|^2 = \sum_j p_j^{(r)} \left|c_j^{(r)}\right|^2,
\tag{42}
$$

which ensures the unitarity of the scattering matrix

$$
\mathbf{S}_E^\dagger \mathbf{S}_E = I.
\tag{43}
$$

Hence, $\det[\mathbf{S}_E] = e^{i2\delta_E}$ and $\frac{1}{2\pi i} \ln\left[\det\left[\mathbf{S}_E\left(\phi_l, \phi_r\right)\right]\right] = \frac{1}{\pi}\delta_E\left(\phi_l, \phi_r\right)$. Numerically, we just need to compute the quantity $\delta_E\left(\phi_l, \phi_r\right)$ and the integral

$$
W\left(\phi_l, \phi_r\right) = \int_{E_{gap}}^\infty \frac{dE}{\pi} \delta_E\left(\phi_l, \phi_r\right).
\tag{44}
$$

The continuum contribution $W\left(\phi_l, \phi_r\right)$ has 2π periodicity in both ϕ_l and ϕ_r, with Fourier decomposition of $W\left(\phi_l, \phi_r\right) = \frac{1}{2}\sum_{n_l,n_r=-\infty}^\infty W_{n_l,n_r} \cos(n_l\phi_\ell + n_r\phi_r)$, with Fourier coefficients of W_{n_l,n_r}. The relevant Fourier components are $J_{L/R} = W_{1,0} = W_{0,1}$, and $J_{Z,2n} = W_{n,n}$ for $n = 1, 2, \cdots$.

There is one subtle issue in the computation of the scattering matrix. There are four propagating modes for $E > \left|B^{(l,r)} + \sqrt{\left(\mu^{(l,r)}\right)^2 + \left(\Delta^{(l,r)}\right)^2}\right|$, but there are two propagating modes and two localized modes for $\left|B^{(l,r)} + \sqrt{\left(\mu^{(l,r)}\right)^2 + \left(\Delta^{(l,r)}\right)^2}\right| > E > E_{gap}^{(l,r)} = \left|B^{(l,r)} - \sqrt{\left(\mu^{(l,r)}\right)^2 + \left(\Delta^{(l,r)}\right)^2}\right|$. In the latter case, we need to compute the effective scattering matrix that are projected to the subspace spanned by the propagating modes.